



Cite this: Dalton Trans., 2016, 45, 16393

Rare-earth metal diisopropylamide-catalyzed intramolecular hydroamination[†]

Tatiana Spallek and Reiner Anwander*

Rare-earth metal diisopropylamide complexes $\text{LiLn}(\text{NPr}_2)_4(\text{THF})$ ($\text{Ln} = \text{Sc, Y, La}$), $[\text{LiY}(\text{NPr}_2)_4]_n$, $\text{NaLn}(\text{NPr}_2)_4(\text{THF})$ ($\text{Ln} = \text{Sc, Y}$), $\text{Sc}(\text{NPr}_2)_3(\text{THF})$ and $\text{Ce}(\text{NPr}_2)_4$ were screened as catalysts for the intramolecular hydroamination/cyclization (IHC) of 1-amino-2,2-dimethyl-4-pentene, 1-amino-2,2-diphenyl-4-pentene, and 1-amino-2,2-diphenyl-5-hexene at ambient and moderately increased temperature of 60 °C in C_6D_6 . The lithium ate complexes displayed the most efficient precatalysts with high conversion rates at 60 °C for the phenyl-substituted substrates and $\text{Ln} = \text{Y}$ and La , affording turnover frequencies N_t as high as 164 h^{-1} . The catalytic activity could be increased by employing THF-free complex $[\text{LiY}(\text{NPr}_2)_4]_n$ ($N_t = 45.8 \text{ h}^{-1}$ at 26 °C; 34.1 h^{-1} for $\text{LiY}(\text{NPr}_2)_4(\text{THF})$). *In situ* generation of putative $\text{LiY}(\text{NPr}_2)_4(\text{THF})$ from $\text{YCl}_3(\text{THF})_{3.3}$ and four equivalents of LiNPr_2 (LDA) in C_6D_6 generated a catalyst revealing N_t comparable to pre-isolated crystallized $\text{LiY}(\text{NPr}_2)_4(\text{THF})$ but yielding even higher substrate conversion. The IHC reactions were also examined for rare-earth metal bis(trimethylsilyl)amide catalysts $\text{Ln}[\text{N}(\text{SiMe}_3)]_3$ ($\text{Ln} = \text{Sc, Y, La}$) as well as for LDA using the same reaction conditions, revealing overall superior activity of the silyl amide derivatives but poor performance of LDA compared to the rare-earth metal diisopropylamide complexes $\text{LiLn}(\text{NPr}_2)_4(\text{THF})$. Cyclization of 1-amino-2,2-diphenyl-5-hexene to the 6-membered heterocycle 2-methyl-4,4-diphenylpiperidine by lanthanum derivative $\text{LiLa}(\text{NPr}_2)_4(\text{THF})$ was accompanied by a competitive isomerization reaction affording max. 20% of 1-amino-2,2-diphenyl-4-hexene after 2 h at 60 °C. Crystalline tetravalent $\text{Ce}(\text{NPr}_2)_4$ showed a better IHC performance than crystalline trivalent $\text{Sc}(\text{NPr}_2)_3(\text{THF})$ as preliminary examined for 1-amino-2,2-diphenyl-4-pentene at 26 °C ($N_t = 5.6$ and 0.9 h^{-1} , respectively), but cyclization came to a halt after 2 h, probably due to decomposition of the catalyst.

Received 1st August 2016,
Accepted 14th September 2016

DOI: 10.1039/c6dt03045a

www.rsc.org/dalton

Introduction

Over the past 25 years, the hydroamination of olefins, and in particular the intramolecular hydroamination/cyclization (IHC) of aminoolefins and aminoalkynes, has developed into a most prominent catalytic reaction in (organo)rare-earth metal chemistry.^{1–5} The IHC affords direct and atom-efficient access to natural products like alkaloids and other functionalized mono- and polyazacycles.^{1–5} The ground breaking discovery by Marks *et al.* in 1989 revealed that rare-earth metallocene-based catalysts of the type $[(\text{C}_5\text{Me}_5)_2\text{LnH}]_2$ or $(\text{C}_5\text{Me}_5)_2\text{LnCH}(\text{SiMe}_3)_2$ convert 2,2-dimethyl-4-penten-1-amine (herein denoted as aminoalkene **S1**) very efficiently into a pyrrolidine derivative (herein denoted as product **P1**), with the catalytic activity being metal-size-dependent (maximum turnover frequencies N_t for lanthanum: 125 and 95 h^{-1} (25 °C), respectively).⁶ Later on, catalyst design put main emphasis on chelating diamido-

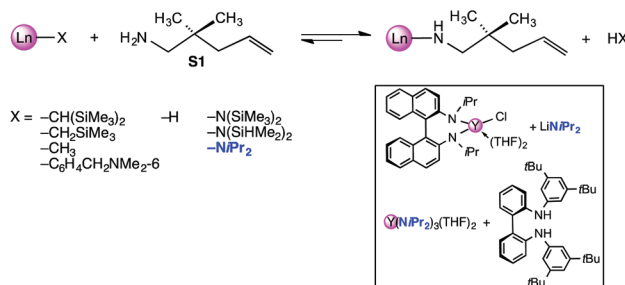
and diaryloxo ancillary ligands L^{2-} as well as on readily exchangeable monoanionic amido ligands NR_2 (= actor ligand) targeting well-defined discrete complexes $\text{LLn}^{\text{III}}\text{NR}_2$.^{4,7–13} Many of these non-metallocene complexes have been accessed *via* protonolysis reactions – often generated *in situ* – using silyl-amide complexes $\text{Ln}[\text{N}(\text{SiMe}_3)_2]_3$ or $\text{Ln}[\text{N}(\text{SiHMe}_2)_3]_3(\text{THF})_x$.^{7,8} More recently, the implementation of chiral variants for asymmetric hydroamination has been successful^{5,9–13} and the feasibility of intermolecular hydroamination has been demonstrated at elevated temperatures.^{4,14}

Ln^{III} precatalysts of the type $\text{L}'\text{Ln}^{\text{III}}(\text{NR}_2)_2$,^{7,9} $\text{Ln}^{\text{III}}(\text{NR}_2)_3$,^{8,15} and $\text{Ln}^{\text{III}}(\text{NR}_2)_4^-$ bearing two, three or four exchangeable monoanionic amido ligands NR_2 , respectively, did receive much less attention. Lack of a rigid stabilizing ancillary ligand backbone, ligand redistribution, and multiple active sites have to be considered potential drawbacks. Nevertheless, the C_2 -symmetric bis(oxazolinato) bis(amido) complex $[(4R,5S)\text{-Ph}_2\text{Box}]\text{La}[\text{N}(\text{SiMe}_3)_2]_2$ exhibited good rates (*e.g.*, **S1**: $N_t = 25 \text{ h}^{-1}$; 23 °C)⁹ and homoleptic $\text{Y}[\text{N}(\text{SiMe}_3)_2]_3$ was advertised as a commercially available comparatively inexpensive precatalyst (*e.g.*, **S1**: $N_t = 11.6 \text{ h}^{-1}$; 25 °C).¹⁵ Moreover, surface grafting of the latter homoleptic derivative on large-pore mesoporous silica afforded hybrid

Institut für Anorganische Chemie, Universität Tübingen, Auf der Morgenstelle 18, 72076 Tübingen, Germany. E-mail: reiner.anwander@uni-tuebingen.de

† Electronic supplementary information (ESI) available: Details of experimental procedures, NMR and catalytic data. See DOI: 10.1039/c6dt03045a





Scheme 1 Protonolysis of the precatalyst as initiating step of the IHC catalytic cycle: scope of routinely employed actor ligands X and relevant examples of diisopropylamide complexes.

material $Y[N(SiMe_3)_2]_3$ @SBA-15-LP₅₀₀ featuring markedly enhanced catalytic activity (e.g., **S1**: $N_t = 36 \text{ h}^{-1}$, 50 °C).¹⁶

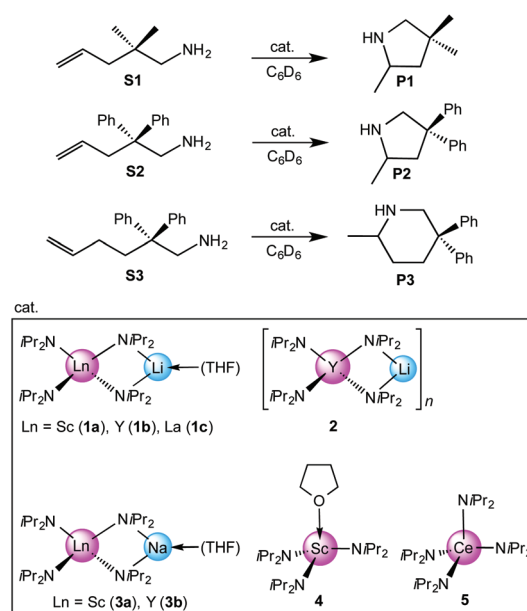
Referring to the initiating step of the IHC catalytic cycle (= X/amine ligand exchange; Scheme 1) it has been pointed out several times that tuning of the actor ligand can be beneficial for enhancing the reaction rate or turnover frequencies (N_t). For diamidoamine complexes $[(2,4,6-\text{Me}_3\text{C}_6\text{H}_2\text{NCH}_2\text{CH}_2)_2\text{NMe}_2]Y\text{X}$ it was found that the least basic actor ligand X = N(SiHMe₂)₂ gave significantly reduced reaction rates (**S1**: $N_t = 1.3 \text{ h}^{-1}$; 40 °C) compared to X = N(SiMe₃)₂ (**S1**: $N_t = 8.4 \text{ h}^{-1}$; 25 °C) and an aryl derivative (X = C₆H₄CH₂NMe₂-6; **S1**: $N_t = 10 \text{ h}^{-1}$; 25 °C).¹⁷ In general, the rate dependence on actor ligands X = N(SiMe₃)₂ versus X = CH(SiMe₃)₂ was less revealing, but for selected ancillary ligand systems, the higher basicity of the silylalkyl ligand gave higher N_t values. Representative examples feature *C*₁-symmetric *ansa*-metallocene complexes Me₂Si(Me₄C₅)(C₅H₃R^{*})LnX (R^{*} = chiral auxiliary, e.g., (+)-neomenthyl; **S1**: $N_t = 21$ versus 38 h⁻¹; 25 °C)¹⁸ or chiral 3,3'-bis(trisaryl)silyl-substituted binaphtholate complexes $R\{[\text{Binol-Si}(3,5\text{-xylyl})_3]\text{LaX}(\text{THF})_2\}$ (**S1**: $N_t = \geq 60$ versus 94 h⁻¹; 22 °C).¹¹ Surprisingly, rare-earth metal alkylamido moieties, e.g., Ln-NiPr₂, have barely been considered as actor ligands, despite of their enhanced basicity/exchangeability (e.g., $pK_{a,\text{THF}} = 22.8$ (HN(SiHMe₂)₂),¹⁹ 35.7 (HN*i*Pr₂)),²⁰ ready availability from LnCl₃(THF)_x and alkali metal amides like lithium diisopropyl amide (LDA),²¹ and inexpensiveness compared to silylamine derivatives.^{‡22–24} In addition, any released isopropylamine during the initial substrate coordination displays a weak donor ligand/nucleophile. In 2003, Scott *et al.* employed discrete *t*Bu-3,5-functionalized bisarylamide silylamine complexes (X = N(SiHMe₂)₂; Ln = Y: **S1** full conversion after 14 d at 60 °C) for enantioselective IHC reactions, but emphasized that use of the more basic diisopropylamido ligand (X = NiPr₂) – precatalyst generated *in situ* via protonolysis of Y(NiPr)₃(THF)₂ (Scheme 1, box) – gave significantly increased turnovers (Ln = Y: **S1** full conversion after 5 d at 35 °C).²⁵ Moreover, the *R*-*N,N*-diisopropyl-1,1'-binaphthyl-2,2'-diamide complex $[(R)\text{C}_2\text{H}_{12}(\text{NiPr})_2]Y(\text{NiPr})_2(\text{THF})\{\text{Li}(\text{THF})_2\}$ (Scheme 1, box),

obtained *via* salt metathesis from the chloro derivative and LDA and used as crude reaction product, proved to be much more reactive than ate complex $[\text{Li}(\text{THF})_4]Y[(R)\text{C}_2\text{H}_{12}(\text{NiPr})_2]_2$.²⁶ Latter ate complexes have been investigated in detail for IHC,^{27–30} and the effect of the alkali metal counterion (Li⁺ *versus* K⁺)²⁸ and the presence of LiCl²⁹ scrutinized. Given the catalytic activity of such 1,1'-binaphthyl-2,2'-diamide ate complexes it seems like an oversimplification to discuss the IHC inactivity of half-sandwich anilide complexes like $[\text{C}_5\text{H}_2(\text{SiMe}_3)_3\text{-}1,2,4]\text{La}(\text{NH}_6\text{H}_3\text{iPr}_2\text{-}1,6)\text{py}_2$ solely on the basis of relative pK_a values while ruling out any effect of halo ligands.³¹ In our preceding study we have described the syntheses and structural chemistry of a series of rare-earth metal diisopropylamide complexes.²¹ Herein we present a comparative study of the catalytic activity of a number of structurally defined rare-earth metal ate complexes, LiLn(NiPr)₄(THF) (Ln = Sc, Y, La) and NaLn(NiPr)₄(THF)₂ (Ln = Sc, Y), donor (THF)-free $[\text{LiY}(\text{NiPr})_4]_n$, as well as of rare-earth metal silyl-amides Ln[N(SiMe₃)₂]₃ (Ln = Sc, Y, La) for the IHC of selected terminal aminoalkenes.

Results and discussion

IHC activity of bimetallic ate complexes LiLn(NiPr)₄(THF)

Because of their easy accessibility for the entire rare-earth metal series, we examined in detail the performance of the bimetallic ate complexes LiLn(NiPr)₄(THF) (Ln = Sc (**1a**), Y (**1b**), La (**1c**)) in the hydroamination/cyclization of terminal aminoalkenes (Scheme 2).



Scheme 2 IHC of terminal aminoalkenes 1-amino-2,2-dimethyl-4-pentene (**S1**), 1-amino-2,2-diphenyl-4-pentene (**S2**), and 1-amino-2,2-diphenyl-5-hexene (**S3**) promoted by rare-earth metal diisopropylamide complexes LiLn(NiPr)₄(THF) (Ln = Sc (**1a**), Y (**1b**), La (**1c**)), $[\text{LiY}(\text{NiPr})_4]_n$ (**2**), NaLn(NiPr)₄(THF) (Ln = Sc (**3a**), Y (**3b**)), Sc(NiPr)₃(THF) (**4**) and Ce(NiPr)₂ (**5**).

[‡] It has been shown that LDA²² or treatment of lithiated aminoalkene with diisopropylamine^{23,24} can efficiently catalyze IHC of non-activated olefins.



It has been previously shown that the substrates amino-2,2-dimethyl-4-pentene (**S1**), 1-amino-2,2-diphenyl-4-pentene (**S2**), and 1-amino-2,2-diphenyl-5-hexene (**S3**) give the cyclized products 2,4,4-trimethylpyrrolidine (**P1**), 2-methyl-4,4-diphenylpyrrolidine (**P2**), and 2-methyl-5,5-diphenylpiperidine (**P3**), respectively.³ The scope of substrates, products and well-defined catalysts under study are illustrated in Scheme 2.

The catalytic reactions have been monitored by ¹H NMR spectroscopy using C₆D₆ as a solvent, and 2 or 4 mol% of pre-catalyst at 26 °C or 60 °C (Table 1). For phenyl-substituted aminoalkenes **S2** and **S3**, the color of the reaction mixtures changed from colourless to yellow at the beginning of the catalytic transformations. The progress of ring closure was determined by the integral ratios of the ¹H NMR specific peaks of the substrates and products relative to the signal of free HNiPr₂. Protonolysis of the NiPr₂ ligands proceeded rapidly after aminoalkene addition to the pre-catalyst solution and stayed constant during the catalytic runs, as already observed by Marks *et al.*^{6b} and others for actor ligand N(SiMe₃)₂.¹⁶

Exemplarily, the progress of the catalytic transformation of substrate **S3** (entry 14) is shown in Fig. S1† and clearly corroborated by the disappearance of the olefinic signals at around 5–6 ppm. The structures/compositions of the products **P1–P4** were assigned by comparison with literature data.³²

Generally, complexes LiLn(NiPr₂)₄(THF) (Ln = Sc (**1a**), Y (**1b**), La (**1c**)) follow the prevailing rules for IHC observed for rare-earth metal catalysts.³ Comparison of entries 1, 5, and 12 (Table 1) shows that the ring closing for the investigated aminoalkenes **S1**, **S2**, and **S3** catalyzed by the same pre-catalyst proceeds according to the Thorpe-Ingold-effect.^{33,34} The rates of cyclization revealed the trends consistent with the Baldwin's guidelines for ring closure,³⁵ meaning that aminoalkene **S1** is the least reactive, while **S2** is easily converted. Furthermore, as previously observed the catalytic activity increased with

increasing ionic radius of the rare-earth metal centre (e.g., Table 1, entries 1, 2, and 4).⁶ Quantitative conversion of aminoalkenes **S2** and **S3** with pre-catalysts **1b** (Y; Table 1, entries 7 and 13) and **1c** (La; Table 1, entry 10) was observed after 0.15 h at 60 °C with the highest N_t = 164 h⁻¹. Therefore, the cyclization of **S2** was additionally monitored at 26 °C. La-catalyst **1c** with the largest rare-earth metal centre is the most efficient displaying 99% conversion after 0.6 h at 26 °C (Table 1, entry 11), followed by Y-catalyst **1b** (Table 1, entry 9) with 88% conversion after 1.5 h. After *ca.* 5 h, the respective Sc-catalyst **1a** had converted only 26% of **S2** (Table 1, entry 6). This latter effect of the rare-earth metal onto the IHC of aminoalkene **S2** is depicted in Fig. 1. The experimental conversion/time data plots for all three aminoalkenes and LiY(NiPr₂)₄(THF) (**1b**) as the pre-catalyst are shown in Fig. 2. Significant transformation of substrate **S1** occurred only at 60 °C. Surprisingly, La complex **1c** did not convert aminoalkene **S3** as efficiently as anticipated and the reactions seemed not completed even after several days (Table 1, entries 17 and 18). Careful analysis of the ¹H NMR spectroscopic data, however, revealed the conformation of isomerized byproduct 1-amino-2,2-diphenyl-4-hexene (**P4**, Fig. 3). The formation of **P4** started parallel to that of the main cyclized product **P3** and reached *ca.* 20% conversion (relative to the concentration of the substrate), independent of the reaction temperature (60 °C or 26 °C). The experimental conversion/time data plots using 4 mol% LiLa(NiPr₂)₄(THF) (**1c**, Table 1, entry 17) are shown in Fig. 4, corroborating that the competitive isomerization reaction for **S3** slowed down markedly the formation of the major cyclized product **P3**. Such concomitant aminoalkene isomerizations were observed previously in IHC reactions employing alkali metal bases such as NaK alloy or n-BuLi,^{23,24} and alkaline-earth metal complexes.³⁶ While the use of NaK gave the isomerized aminoalkene as the major product, treatment of amino-2,2-dimethyl-4-pentene

Table 1 IHC of aminoalkenes **S1–S3** catalyzed by LiLn(NiPr₂)₄(THF) (**1**)^a

Entry	Aminoalkene	Product	Catalyst	T/°C	t/h	Conv./% ^b	N _t /h ⁻¹
1			1a (Sc)	60	4.84	<1	<1
2			1b (Y)	60	4.84	24	1.6/1.2 ⁱ
3 ^d			1b (Y)	60	9.7	<1	<1
4			1c (La)	60	4.84	47	18.1/2.9 ⁱ
5			1a (Sc)	60	1.0	43	10.6/5.2
6			1a (Sc)	26	4.84	26	3.3/1.4 ⁱ
7			1b (Y)	60	0.15	>99	—/164
8 ^d			1b (Y)	60	0.6	>98	88/90
9			1b (Y)	26	1.5	>88	67.3/34.1
10			1c (La)	60	0.15	>99	—/164
11			1c (La)	26	0.6	>99	151.4/4 ^g
12			1a (Sc)	60	2.27	>99	21.8/14.7
13			1b (Y)	60	0.15	>99	—/164
14 ^d			1b (Y)	60	0.9	>99	69.0 ^h
15			1b (Y)	26	2.12	>99	13.6/11.3
16 ^d			1b (Y)	26	4.84	36	5.4/4.3 ⁱ
17			1c (La)	60	4.84	>99 ^e	15.5/9.7
18			1c (La)	26	288	>98 ^e	0.2/0.1 ⁱ

^a 4 mol% **1** in C₆D₆. ^b All conversion data were derived from ¹H NMR spectra referring to the corresponding duration of reaction. ^c Initial N_t versus overall N_t (taken at 80% conversion, unless otherwise stated). ^d 2 mol% **1b** in C₆D₆. ^e Ratio cyclized product **P3**: isomerized aminoalkene **P4** ≈ 4 : 1. ^f Conversion completed after <9 min. ^g At 99% conversion. ^h Initial N_t = N_t at 80%. ⁱ N_t at time t given in this table.



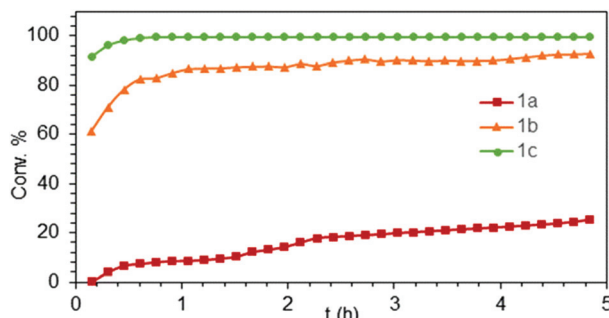


Fig. 1 Experimental conversion/time data plots for the IHC of aminoalkene **S2** at 26 °C by using 4 mol% $\text{LiLn}(\text{NiPr}_2)_4(\text{THF})$ ($\text{Ln} = \text{Sc}$ (**1a**, Table 1, entry 6), **Y** (**1b**, Table 1, entry 9), La (**1c**, Table 1, entry 11)) as precatalysts.

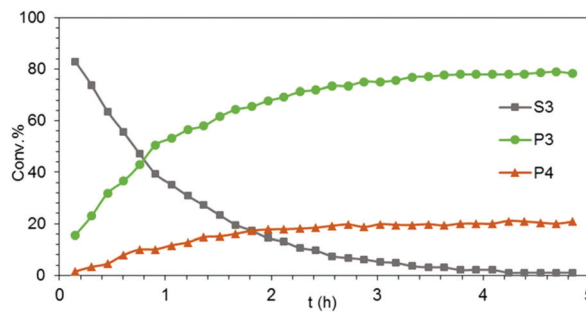


Fig. 4 Experimental conversion/time data plots for the transformation of aminoalkene **S3** into cyclized main product **P3** and isomerized side product **P4** using 4 mol% $\text{LiLa}(\text{NiPr}_2)_4(\text{THF})$ as precatalyst (Table 1, entry 17).

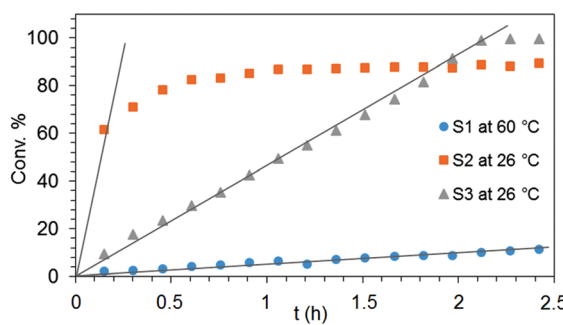


Fig. 2 Experimental conversion/time data plots for the IHC of aminoalkenes **S1** at 60 °C (Table 1, entry 2), **S2** at 26 °C (Table 1, entry 9) and **S3** at 26 °C (Table 1, entry 15) by using 4 mol% $\text{LiY}(\text{NiPr}_2)_4(\text{THF})$ as precatalyst.

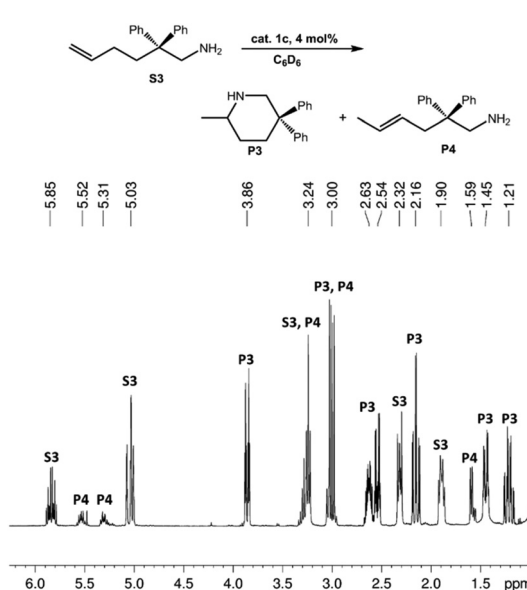


Fig. 3 ^1H NMR spectrum (shown in the region 1.0–6.2 ppm) of the catalytic IHC and isomerization reactions of 1-amino-2,2-diphenyl-5-hexene (**S3**) to main product 2-methyl-5,5-diphenylpiperidine (**P3**) and isomerized side product 1-amino-2,2-diphenyl-4-hexene (**P4**) using La-catalyst **3c** (Table 1, entry 17).

(**S1**) with *n*-butyllithium in THF led to cyclization.²³ Later, Markó *et al.* treated 1-amino-4-pentene with 16 mol% *n*-BuLi which led to the cyclization product, but the isomerized alkene formed to different extents.²⁴ A detailed investigation and discussion of the formation of isomerized aminoalkene in the course of IHC was performed by Hill *et al.* for the cyclization of 1-amino-2,2-dimethyl-5-hexene and 1-amino-2,2-diphenyl-5-hexene (**S3**) in the presence of the β -diketiminato-supported calcium complex $\{[\text{ArNC(Me)}\text{CHC(Me)}\text{NAr}]\text{Ca}[\text{N}(\text{SiMe}_3)_2](\text{THF})\}$.^{36a} For the **S3**-reaction, the *ca.* 10% yield of the isomerized byproduct (which was not observed for the magnesium precatalyst $\{[\text{ArNC(Me)}\text{CHC(Me)}\text{NAr}]\text{MgMe}(\text{THF})\}$) were ascribed to stereoelectronic effects: formation of a boat-like six-membered ring transition state might lead to an allyl species *via* intramolecular proton transfer and subsequently to the isomerized product **P4** (or regenerated **S3**) *via* protonolysis.^{36a} To the best of our knowledge such competitive isomerization/IHC reactions have not been observed yet for rare-earth metal catalysts.³⁷ Any competing effect of the lithium cation might be ruled out on the basis of a VT NMR study since the $\text{Li}(\text{THF})^+$ fragment shows approximately the same mobility in the respective yttrium (**1b**) and lanthanum complexes (**1c**).²¹

As in the case of the aforementioned Mg/Ca transformations, the occurrence of the isomerization reaction in the presence of $\text{LiLa}(\text{NiPr}_2)_4(\text{THF})$ (**1c**) can be rationalized on the basis of the large size of La(III). In this sense the scandium (**1a**) and yttrium (**1b**) catalysts did not yield any detectable amount of **P4**.^{36a} Similar to the study by Hill *et al.* the isomerized byproduct does not undergo subsequent cyclization. Overall, the distinct reactivity of **1c** toward **S3**, which is comparable to that of $\{[\text{ArNC(Me)}\text{CHC(Me)}\text{NAr}]\text{Ca}[\text{N}(\text{SiMe}_3)_2](\text{THF})\}$ seems to originate from similarities of the calcium(II) and lanthanum(III) cations *e.g.*, Lewis acidity³⁸ and comparable size of the effective ionic radii (Ca^{2+} 1.00–1.34 Å and La^{3+} 1.03–1.36 Å, depending on the coordination number).³⁹ Precatalyst **1c** did not promote the isomerization of aminoalkene **S1** and **S2**.

IHC catalytic activity of LDA

Early research on the generation of carbon–nitrogen bonds involved the alkali metal-catalyzed amination of olefins in

Table 2 IHC of aminoalkene **S2** and **S3** promoted by LDA at variable concentrations and temperatures in C_6D_6

Entry	Aminoalkene	Product	Conc./mol%	T/°C	t/h	Conv./% ^a	N_t^b/h^{-1}
1			4	60	96	<1	<1 ^c
2			12	26	4.84	18	1.9/0.3 ^c
3			21	60	96	43	<0.1
4			4	26	4.84	>99	1.2/1.2

^a All conversion data were derived from 1H NMR spectra referring to the corresponding duration of reaction. ^b Initial N_t versus overall N_t (taken at 80% conversion, unless otherwise stated). ^c N_t at time t given in this table.

1957⁴⁰ and 1985.⁴¹ The application of LDA supported by irradiation (150 W tungsten bulb) was described by Trost *et al.* as a viable protocol in alkaloid synthesis.⁴² Moreover, Markó *et al.* reported on the addition of diisopropylamine to the lithiated substrate 1-amino-4-pentene or treatment with either catalytic quantities or with 1 equiv. of LDA to afford the cyclized product 2-methylpyrrolidine.²⁴ Furthermore, mixtures of *n*-BuLi/HNiPr₂⁴³ and LiN(SiMe₃)₂/TMEDA,⁴⁴ as well as a chiral lithium amides⁴⁵ were successfully utilized in base-catalyzed IHC reactions. In order to exclude any significant effect of LDA, the separation of which might occur in ate complex (**1**)/substrate (**S**) reaction mixtures, we probed the IHC catalytic activity of LDA for the aminoalkenes under study. Putative cyclization of **S2**, which benefits most from the Thorpe-Ingold effect, did not occur in the presence of 4 mol% LDA even after 96 h at 60 °C (Table 2, entry 1). The formation of a significant amount of cyclized product **P2** (*ca.* 18%) could be observed after 5 h, using 12 mol% LDA at 26 °C (Table 2, entry 2). Further increase of both the reaction temperature (60 °C) and concentration of LDA (21 mol%) led to full conversion of substrate **S2** after 4 h (Table 2, entry 3).

As mentioned in the introduction, the only known rare-earth metal ate complexes, which have been investigated in detail for the catalytic IHC, are bimetallic lanthanide-binaphthylamide complexes of the **A** and **B**-type (Chart 1).^{27–29,46,47} While addition of LiCl to $[(R)-C_{20}H_{12}(NR)_2]Y(CH_2SiMe_3)(THF)_2$ and $[(R)-C_{20}H_{12}(NR)_2]Y(NiPr_2)(THF)_2$ ($R = c-C_5H_9$, SiMe₃, SiMe₂tBu) mainly produced higher enantioselectivities,²⁹ lithium-ate complexes $[(Li(THF)_4)Ln[(R)-C_{20}H_{12}(NR)_2]_2$ displayed higher catalytic activity than the potassium analogues $[K(THF)_5]Ln[(R)-C_{20}H_{12}(NR)_2]$ ($Ln = Y$, Yb; $R = c-C_5H_9$, CH₂tBu).²⁸ It is noteworthy that such bimetallic rare-earth metal binaphthylamide complexes were employed to some extent generated *in situ*⁴⁸ and required higher concentrations of the catalysts and longer reaction times²⁸ compared to our ate complexes LiLn(NiPr₂)₄(THF). Diethylamide ate complexes of type **C** (Chart 1) were described as efficient catalysts for asymmetric IHC reactions.^{12a}

The Li/Y diisopropylamide catalyst system

The IHC activity of complex LiY(NiPr₂)₄(THF) (**1b**) was further elaborated at a concentration of 2 mol% (*cf.*, Table 1).

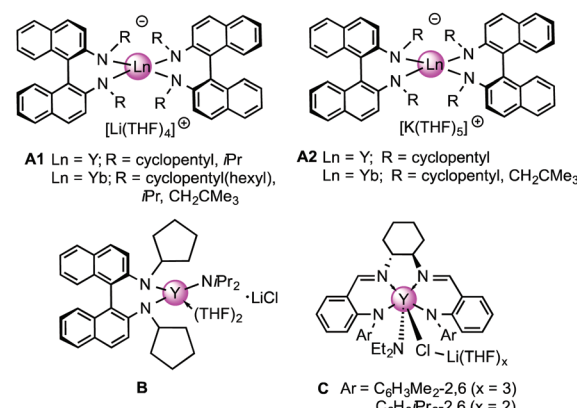


Chart 1 Bimetallic rare-earth metal ate complexes previously employed as precatalysts for (asymmetric) IHC reactions.

Compared to the 4 mol%-reaction, which gave 24% conversion of **S1** after 4.84 h at 60 °C (Table 1, entry 2), use of half of the amount of **1b** did not produce any detectable **P1** even after 9.7 h (Table 1, entry 3). In contrast, under the same conditions 98% of aminoalkene **S2** were converted after 0.6 h (Table 1, entry 8) and, similarly, aminoalkene **S3** could be cyclized after 0.9 h (Table 1, entry 14). At 26 °C, cyclization of **S3** in the presence of 2 mol% **1b** was noted at 36% after 4.84 h (Table 1, entry 16). These results underline the high catalytic activity of the investigated amide complexes, the impact of the Thorpe-Ingold effect, as well as the different rates of the formation of five- and six-membered rings. The experimental conversion/time data plots for the IHC of aminoalkenes **S2** and **S3** using 2 mol% **1b** as the precatalyst are depicted in Fig. 5.

In our preceding work on rare-earth metal diisopropylamide complexes, the diversity of molecular compositions, solution behaviours and solid-state structures depending on the ratio $MNiPr_2/LnCl_3$ ($M = Li, Na$) and presence of donor solvent was emphasized.²¹ In the following experiments we assessed the catalytic performance of (a) $[LiY(NiPr_2)_4]_n$ (2), that is, in the absence of donor solvent THF (Table 3, entry 3), (b) *in situ* generated bimetallic catalysts using $LiNiPr_2/LnCl_3$ ratios of 4 (aiming at **1b**; Table 3, entry 4) and 2.5 (aiming at $Y(NiPr_2)_3(THF)_x$; Table 3, entry 5), (c) *in situ* generated

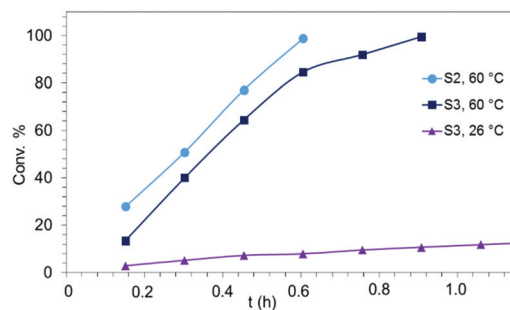


Fig. 5 Experimental conversion/time data plots for the IHC of aminoalkenes **S2** and **S3** using 2 mol% $\text{LiY}(\text{NiPr}_2)_4(\text{THF})$ (**1b**) as precatalyst (Table 1, entries 8, 14, and 16).

$\text{LiY}[\text{N}(\text{SiHMe}_2)_2]_4(\text{THF})$ (from $\text{YCl}_3(\text{THF})_{3.3} + 4 \text{LiN}(\text{SiHMe}_2)_2$) (Table 3, entry 6), and (d) crystalline $\text{NaY}(\text{NiPr}_2)_4(\text{THF})$ (**3b**) to probe any alkali metal effect, compared to pure crystalline complex **1b** (Table 1, entry 9) and LDA (Table 2, entry 2).

(a) Indeed, the THF-free polymeric complex $[\text{LiY}(\text{NiPr}_2)_4]_n$ (**2**), which is soluble in aliphatics and aromatics, revealed the highest catalytic activity of all isopropylamide complexes under study (Fig. 6). Using 4 mol% of **2** the conversion of **S2** was completed after 1.1 h even at ambient temperature (Table 3, entry 3 and Fig. 6). The superior reactivity of **2** compared to the THF-coordinate congeners **1b** (Table 1, entry 9 and Fig. 6) can be rationalized on the basis of their distinct dynamic behaviours in solution as revealed by VT NMR spectroscopic studies, suggesting distinct Li–N bonding in **2**. This might affect the intitial protonolysis reaction (NiPr_2 /substrate exchange, Scheme 1). Moreover, upon elimination of a bulky NiPr_2 ligand the Lewis base THF present in **1b** could switch from Li to Y coordination and thus compete with any vacant coordination site of the catalyst, the availability of which is essential for the subsequent insertion/cyclization step of the catalytic cycle. The IHC reaction of **S2** catalyzed by **2** was repeated under the same conditions using 5.09 μmol of

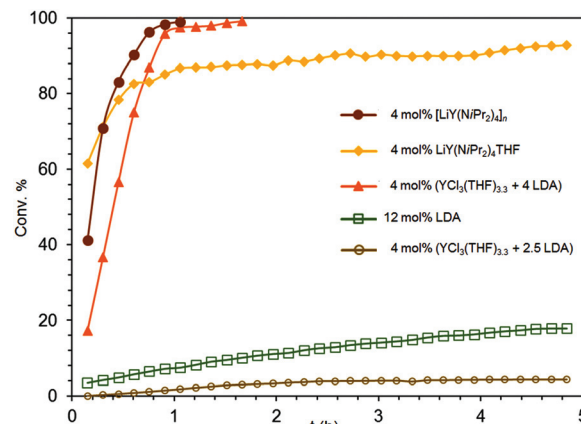


Fig. 6 Experimental conversion/time data plots for the IHC of aminoalkene **S2** promoted by 4 mol% $\text{LiY}(\text{NiPr}_2)_4(\text{THF})$ (**1b**), 12 mol% LDA, 4 mol% $[\text{LiY}(\text{NiPr}_2)_4]_n$ (**2**), 4 mol% $\text{YCl}_3(\text{THF})_{3.3}/4$ LDA, and 4 mol% $\text{YCl}_3(\text{THF})_{3.3}/2.5$ LDA (cf., Table 3, entries 1–5).

tetrakis(*p*-tolyl)silane as an internal standard revealing the same conversion and NMR yield >99% after 1.1 h (initial $N_t = 62.4 \text{ h}^{-1}$ and overall $N_t = 45.92 \text{ h}^{-1}$ at 80% conversion (Fig. S2†)). The negative effect of THF on IHC reactions was early observed by Marks *et al.*⁶

(b) More interestingly, isolation and crystallization of complexes **1b** or **2** seem not be a prerequisite for efficiently catalyzing the IHC reaction. Although crystalline complex **1b** afforded 78% conversion of **S2** after 0.5 h, the reaction decelerated drastically afterwards (Table 1, entry 9 and Fig. 6). The corresponding reaction employing the respective *in situ* generated catalyst, preformed from $\text{YCl}_3(\text{THF})_{3.3}$ and 4 equivalents of LiNiPr_2 in C_6D_6 (preformation time 5 min), was at the beginning slower, but afforded 97% conversion of the substrate already after 1 h (Table 3, entry 4 and Fig. 6). It is noteworthy that for both reactions *ca.* 80% cyclization was accomplished

Table 3 IHC of aminoalkene **S2** catalyzed by various amide complexes in C_6D_6 at 26 °C

Entry	Catalyst	Conc./mol%	t/h	Conv./% ^a	N_t ^b /h ⁻¹
1 ^c	$\text{LiY}(\text{NiPr}_2)_4(\text{THF})$ (1b)	4	1.5	>88	67.3/34.1
2 ^d	LDA	12	4.84	18	1.9/0.3 ^e
3 ^f	$[\text{LiY}(\text{NiPr}_2)_4]_n$ (2)	4	1.1	>99	60.5/45.8
4	<i>In situ</i> 1b ($\text{YCl}_3(\text{THF})_{3.3} + 4 \text{ LDA}$)	4	1.7	>99	30.6/28.7
5	<i>In situ</i> $\text{Y}(\text{NiPr}_2)_3(\text{THF})_2$ [$\text{YCl}_3(\text{THF})_{3.3} + 2.5 \text{ LDA}$]	4	4.84	4	0.2 ^e
6	<i>In situ</i> $\text{LiY}[\text{N}(\text{SiHMe}_2)_2]_4(\text{THF})$ [$\text{YCl}_3(\text{THF})_{3.3} + 4 \text{ LiN}(\text{SiHMe}_2)_2$]	4	192	34	<0.1 ^e
			288	47	
7	$\text{Sc}(\text{NiPr}_2)_3(\text{THF})$ (4)	4	4.84	18	4.5/0.9 ^e
8	$\text{Ce}(\text{NiPr}_2)_4$ (5)	4	2.0	44	17.7/5.6 ^e

^a All conversion data were derived from ^1H NMR spectra referring to the corresponding duration of reaction. ^b Initial N_t versus overall N_t (taken at 80% conversion, unless otherwise stated). ^c cf., Table 1, entry 9. ^d cf., Table 2, entry 2. ^e N_t at time t given in this table. ^f The presence of 10 equivalents of HNiPr_2 did not affect the catalytic transformation.

after 0.75 h (see Fig. 6). In contrast, *in situ* generated $\text{Y}(\text{NiPr}_2)_3(\text{THF})_x$, obtained from $\text{YCl}_3(\text{THF})_{3.3}$ and 2.5 equivalents of LiNiPr_2 in C_6D_6 ,²¹ displayed only minor catalytic activity (Table 2, entry 5 and Fig. 6). Applying 4 mol% of the catalyst, only 4% conversion of **S2** was detected after 3 h followed by a stagnation of the IHC reaction. As importantly for assessing the role of LDA is the fact that pure LDA promotes the IHC of substrate **S2** not until a concentration of 12 mol% (Table 2). Moreover, crystallized mixed NiPr_2/Cl complexes such as choro-bridged $[\text{Ln}(\text{NiPr}_2)_2(\mu\text{-Cl})(\text{THF})]_2$ displayed generally lower IHC catalytic reactivity for aminoalkene **S2**. For example, $[\text{Sc}(\text{NiPr}_2)_2(\mu\text{-Cl})(\text{THF})]_2$ converted 31% of the substrate after 48 h (not displayed in Table 3), accounting for a smaller catalytic efficiency per metal centre, compared to catalysts **1a** and **4** (*vide supra*).

(c) Yttrium complexes featuring the less basic but similarly sized bis(dimethylsilyl)amido ligand have been employed previously for catalytic IHC reactions.¹⁷ For direct comparison, $\{\text{LiY}[\text{N}(\text{SiHMe}_2)_2]_4(\text{THF})\}^{49}$ was generated *in situ* from $\text{YCl}_3(\text{THF})_{3.3}$ and four equivalents of $\text{LiN}(\text{SiHMe}_2)_2$ in C_6D_6 (preformation time 5 minutes) (Table 3, entry 6). Not unexpectedly, cyclization of **S2** proceeded very slowly at ambient temperature, affording 34% conversion after 8 d and 47% after another 4 d.

(d) Having synthesized the sodium congeners $\text{NaLn}(\text{NiPr}_2)_4(\text{THF})$ ($\text{Ln} = \text{Sc}$ (**3a**), Y (**3b**)) as well,²¹ we were also interested in elucidating the effect of the alkali metal ion on the IHC reactions (Table S1†). We found that the Y-Na catalyst **3b** exhibits markedly lower activity than the Y-Li catalyst **1b**, converting 37% of **S2** after a reaction time of 3 h at 60 °C and achieving full conversion only after 24 h (Table S1,† entry 2) (**1b**: complete conversion after 9 minutes) (Table 1, entry 7). The decreased catalytic activity of the Y-Na derivative **3b** was further supported by the outcome of the cyclization of substrate **S3** (Table S1†), which gave 15% and complete cyclization after 3 h and 48 h at 60 °C, respectively (Table S1,† entry 4), (**1b**: complete conversion after 9 minutes (Table 1, entry 13)). The decreased reactivity of the sodium ate complexes might originate from their changed dynamic behaviour in solution and decreased thermal stability. A VT NMR spectroscopic study revealed that complex **3b** is highly fluxional even at *ca.* −70 °C (**1b**: above *ca.* 0 °C), which was attributed to a weaker (ionic) bonding of the $\text{Na}(\text{THF})^+$ fragment with the amido ligands compared to the $\text{Li}(\text{THF})^+$ fragment.²¹ The comparatively weaker bonding of the $\text{Na}(\text{THF})^+$ fragment might exert a destabilizing effect on the $\text{Ln}(\text{NiPr}_2)_4^-$ counterion as revealed by accelerated decomposition (formation of HNiPr_2 ; see also ref. 28: Li^+ *versus* K^+). As observed for complexes $\text{LiLn}(\text{NiPr}_2)_4(\text{THF})$ (**1**), the Sc-Na derivative **3a** was far less active than the Y-Na complex **3b**. Complex **3a** converted only traces of the substrates **S2** and **S3** after 24 h reaction time and reached full conversion after 3 and 12 d, respectively (Table S1,† entries 1 and 3). Although the catalytic role and influence of the alkali metals in such bimetallic complexes is not clarified until now, their presence and type clearly affects the catalytic performance of amide complexes. Similar observations were made by Schulz

et al. when probing bimetallic rare-earth metal binaphthyl-amide complexes of the type $[\text{M}(\text{THF})_n\text{Ln}[(R)\text{-C}_2\text{H}_{12}(\text{NR})_2]_2$ ($\text{M} = \text{Li, K}$) as catalysts for IHC.²⁸

IHC catalytic activity of complexes $\text{Sc}(\text{NiPr}_2)_3(\text{THF})$ (**4**) and $\text{Ce}(\text{NiPr}_2)_4$ (**5**)

Crystalline alkali-metal free tris(amido) complex $\text{Sc}(\text{NiPr}_2)_3(\text{THF})$ (**4**) can be readily obtained.²¹ Although it is routinely observed that scandium catalysts are less active than their yttrium counterparts, complex **4** had converted 18% of **S2** after 5 h (Table 3, entry 7) thus kind of outperforming *in situ* formed $\text{Y}(\text{NiPr}_2)_3(\text{THF})_x$, which cyclized 4% during the same time period (Table 3, entry 5). The inefficiency of the latter yttrium-reaction, however, might be also a result of the *in situ* protocol applied for the synthesis of $\text{Y}(\text{NiPr}_2)_3(\text{THF})_x$,⁵⁰ allowing a pre-formation time of 5 min only. Matching the present results, complex **4** is significantly less active than lithium ate complex $\text{LiSc}(\text{NiPr}_2)_4(\text{THF})$ (**1a**) (Table 1, entry 6). Next, we initially probed the IHC catalytic activity of the alkali-metal-free homoleptic tetravalent complex $\text{Ce}(\text{NiPr}_2)_4$ (**5**).⁵¹ Like complexes $\text{LiLn}(\text{NiPr}_2)_4(\text{THF})$ (**1**), the cerium complex **5** adopts a tetrahedral coordination geometry, but features a more Lewis-acidic rare-earth metal center and shorter Ln-N(amido) bonds as a consequence of the tetravalent oxidation state. Generally, there exist only a few reports on molecular organo-Ce(IV) catalysis.⁵² Complex **5** achieved 44% conversion of substrate **S2** after 2 h, displaying an $N_t = 5.6 \text{ h}^{-1}$ (Table 3, entry 8). By then the color of the reaction mixture changed from blue to brown and the cyclization came to an halt, probably due to decomposition of the catalyst.

IHC catalytic activity of rare-earth metal diisopropylamide complexes compared to bis(trimethylsilyl)amides $\text{Ln}[\text{N}(\text{SiMe}_3)_2]_3$

The final part of this study compares the catalytic activities of the investigated rare-earth metal diisopropylamide complexes with those of the ubiquitous rare-earth metal bis(trimethylsilyl)amides $\text{Ln}[\text{N}(\text{SiMe}_3)_2]_3$ ($\text{Ln} = \text{Sc}$ (**6a**), Y (**6b**), and La (**6c**)). Complexes **6** were previously found to efficiently catalyze the IHC of aminoolefins and aminoalkynes.^{8,15} For direct comparison the reactions with precatalysts **6**, which were sublimed prior to use, were carried out using exactly the same conditions as for $\text{LiLn}(\text{NiPr}_2)_4(\text{THF})$ ($\text{Ln} = \text{Sc}$ (**1a**), Y (**1b**), and La (**1c**)) described above. The obtained results as listed in Table 4 are compared in the following with entries 1, 2, 4, 5, 7, 10, 12, 13, and 17 of Table 1. The majority of the reactions revealed that the rare-earth metal bis(trimethylsilyl)amide complexes **6** exhibit overall higher cyclization rates independent of the substrate. In the case of substrate **S3**, an activity increase from **6a** (Sc) to **6c** (La) could be observed as expected (Table 4, entries 7–9) but **6a** afforded almost the same N_t as scandium ate complex **1a** (Table 1, entry 12). It also occurred for **S3**, that the yttrium diisopropylamide complex outperformed the silyl-amide one (**1b**: $N_t = 164 \text{ h}^{-1}$ (Table 1, entry 13); **6b**: $N_t = 13.9 \text{ h}^{-1}$ (Table 4, entry 8)). Moreover, the competitive isomerization reaction of **S3** to give **P4** (Fig. 3 and 4) detected for $\text{LiLa}(\text{NiPr}_2)_4(\text{THF})$ (**1c**) could not be observed for $\text{La}[\text{N}(\text{SiMe}_3)_2]_3$



Table 4 IHC of aminoalkenes catalyzed by $\text{Ln}[\text{N}(\text{SiMe}_3)_2]_3$ (**6**)^a

Entry	Aminoalkene	Product	catalyst	T/°C	t/h	Conv./% ^b	N_t ^c /h ⁻¹
1			6a (Sc)	60	4.84	—	—
2			6b (Y)	60	2.0	>99	37.2/17.1
3			6c (La)	60	1.0	>99	49.1/42.6
4			6a (Sc)	26	0.17	>99	— ^d /149
5			6a (Y)	26	0.17	>99	— ^d /149
6			6b (La)	26	0.17	>99	— ^d /149
7			6a (Sc)	60	2.3	>99	64.3/22.5
8			6b (Y)	60	1.5	>99	13.9 ^e
9 ^f			6b (Y)	26	4.84	traces	—
10			6b (La)	60	1.1	>99	17.4 ^e

^a 4 mol% **6** in C_6D_6 . ^b All conversion data were derived from ^1H NMR spectra referring to the corresponding duration of reaction. ^c Initial N_t versus overall N_t (taken at 80% conversion, unless otherwise stated). ^d Conversion completed after <10 min. ^e Initial $N_t = N_t$ at 80%. ^f Unsublimed **6b**.

(**6c**) which efficiently produced cyclized **P3** (Table 4, entry 10). It is noteworthy that unsublimed $\text{Y}[\text{N}(\text{SiMe}_3)_2]_3$ (**6b**) gave only traces of cyclized product **P3** after 4.84 h at 26 °C (Table 4, entry 9) but full conversion was reached after 4 days. The overall better catalytic performance of the bis(trimethylsilyl) amide derivatives can be rationalized on the basis of less sterically saturated $\text{Ln}(\text{m})$ centres (4- versus 3-coordinate) allowing better initial access of the substrate molecules. Although diisopropylamine displays a similar basicity as the substrate molecules (pK_a values of protonated amines in H_2O : $\text{HNiPr}_2 = 11.05$; primary amines = ca. 10; cyclized products pyrrolidine = 11.27 and piperidine = 11.22) the addition of 10 equivalents of HNiPr_2 to the reaction system **S2/2** did not affect the IHC transformation significantly, arguing against an enhanced coordination capability compared to the silylamine.^{53,54} §

Conclusions

Easily available rare-earth metal diisopropylamide complexes $\text{LiLn}(\text{NiPr}_2)_4(\text{THF})$ ($\text{Ln} = \text{Y, La}$)²¹ display high catalytic activity for regio-selective intramolecular hydroamination/cyclization reactions of terminal aminoalkenes depending on the substrate and the rare-earth metal centre at mild temperatures and low catalyst concentrations. The catalysts can be conveniently obtained *in situ* combining $\text{YCl}_3(\text{THF})$ ^{3,3} and four equivalents of LiNiPr_2 (LDA), briefly before addition of amino-alkene substrate. Although the largest rare-earth metal centre exhibits the highest IHC activity it is prone to side reactions as shown for a competitive isomerization reaction in case of 1-amino-2,2-diphenyl-5-hexene (formation of 1-amino-2,2-diphenyl-4-hexene *versus* the 6-membered heterocycle 2-methyl-4,4-diphenylpiperidine). The occurrence of such iso-

merization reactions in tandem with hydroamination was previously reported for alkali and alkaline-earth metal-promoted catalysis but not in the case of rare-earth metal catalysis. Moreover, the present diisopropylamide case study clearly revealed the effect of donor solvent (THF), halo co-ligands and alkali metals on the catalytic performance of the rare-earth metal complex. It is shown that the presence of THF slows down drastically substrate conversion ($\text{LiLn}(\text{NiPr}_2)_4(\text{THF})$ *versus* $[\text{LiLn}(\text{NiPr}_2)_4]_n$), most likely by competing with substrate coordination/cyclization at the catalytically active centre. Similarly, the presence of highly mobile $\text{AM}(\text{THF})^+$ fragments decelerates the conversion rates (AM = alkali metal; $\text{LiLn}(\text{NiPr}_2)_4(\text{THF}) \gg \text{NaLn}(\text{NiPr}_2)_4(\text{THF})$). The presence of chloro ligands seems to counteract an efficient catalytic process as well as shown for heteroleptic complex $[\text{Sc}(\text{NiPr}_2)_2(\mu\text{-Cl})(\text{THF})]_2$. Compared to the ubiquitous rare-earth metal bis(trimethylsilyl)amides $\text{Ln}[\text{N}(\text{SiMe}_3)_2]_3$ ($\text{Ln} = \text{Sc, Y, La}$), which require sublimation prior to use, the investigated rare-earth metal diisopropylamide complexes show significantly lower catalytic activity. Exceptionally, 4-coordinate complex $\text{LiY}(\text{NiPr}_2)_4(\text{THF})$ outperformed three-coordinate $\text{Ln}[\text{N}(\text{SiMe}_3)_2]_3$ for the IHC of 1-amino-2,2-diphenyl-5-pentene. We assume that the enhanced steric saturation of the rare earth-metal centre in ate complexes $\text{AMLn}(\text{NiPr}_2)_4(\text{THF})_x$ and enhanced thermal instability compared to $\text{Ln}[\text{N}(\text{SiMe}_3)_2]_3$ overcompensate the comparatively higher reactivity of the $\text{Ln}-\text{NiPr}_2$ bond (*versus* $\text{Ln}-\text{N}(\text{SiMe}_3)_2$). Nevertheless, ate complexes $\text{AMLn}(\text{NiPr}_2)_4(\text{THF})_x$ display an overall higher IHC efficiency than the previously reported rare-earth metal diamidobinaphthyl ate complexes.^{27–29,47,48} Finally, our preliminary observations that tetravalent cerium complex $\text{Ce}(\text{NiPr}_2)_4$ revealed higher conversion rates than $\text{Sc}(\text{NiPr}_2)_3(\text{THF})$ might significantly broaden the scope of cerium(IV) catalysis.

Experimental section

General considerations

All operations were performed with rigorous exclusion of air and moisture, using standard Schlenk, high-vacuum, and glovebox

§ Stoichiometric reactions, similarly examined by Piers *et al.*,⁵⁴ performed overnight at 26 °C and involving mixtures $\text{Y}[\text{N}(\text{SiMe}_3)_2]_3/\text{S3}$, $\text{LiSc}(\text{NiPr}_2)_4(\text{THF})/4\text{ S2}$ and $\text{LiNiPr}_2/\text{S2}(\text{S3})$ led to the complete disappearance of the olefinic and NH protons of the substrates, suggesting conversion to the cyclized product which remains coordinated to the metal centre. Unfortunately, several attempts to obtain single crystals of the ligand exchanged products were unsuccessful.



techniques (MB Braun MB150B-G; <1 ppm O₂, <1 ppm H₂O). *n*-Hexane, *n*-pentane, and THF were purified by using Grubbs columns (MBraun SPS, Solvent Purification System) and stored in a glovebox. *n*-Butyllithium (2.5 M in *n*-hexane) and diisopropylamine (99.95%), isobutynitrile (99.6%), allyl bromide (99%), lithium aluminium hydride (95%), 4-bromo-1-butene (97%), and tetrakis(*p*-tolyl)silane (99%) were obtained from Sigma-Aldrich, diphenylacetonitrile (99%) was obtained from ABCR. Benzene-*d*₆ (99.6%) was received from Sigma Aldrich, dried over NaK alloy for a minimum of 48 h, and filtered twice through a filter pipette (Whatman) before use. Chloroform-*d* was obtained from Eurisotop and used as received. Complexes LiLn(NiPr₂)₄(THF) (Ln = Sc (**1a**), Y (**1b**), La (**1c**)), [LiY(NiPr₂)₄]_n (**2**), NaLn(NiPr₂)₄(THF) (Ln = Sc (**3a**), Y (**3b**)) and Sc(NiPr₂)₃(THF) (**4**) were synthesized as described previously.²¹ Complexes Ce(NiPr₂)₄ (**5**),⁵¹ Ln[N(SiMe₃)₂]₃ (Ln = Sc (**6a**), Y (**6b**), La (**6b**)),⁵⁵ and LDA⁵⁶ were synthesized according to literature procedures. Ln[N(SiMe₃)₂]₃ were sublimed twice prior to use. NMR spectra were recorded by using J. Young valve NMR tubes and obtained on a Bruker AVII+400 (¹H: 400.11 MHz, ¹³C: 100.61 MHz), and on a Bruker AVII+500 (¹H: 500.13 MHz) spectrometer. ¹H and ¹³C signals are referenced to internal solvent resonances and reported in parts per million relative to TMS. All NMR spectra of the cyclized products were obtained by *in situ* NMR scale catalytic hydroamination/cyclization reactions of the corresponding aminoalkene with the appropriate precatalyst under the reported conditions.

Representative IHC procedure

In a glovebox, the desired amount of precatalyst or appropriate mixture of the *in situ* generated catalyst were introduced in a J. Young NMR tube and 0.4 mL benzene-*d*₆ was added. The mixture was frozen at -35 °C and a solution of the aminoalkene (0.28 mmol) in 0.3 mL benzene-*d*₆ was injected onto the solid mixture (= *t*₀). The tube was sealed and frozen again. Then, the tube was removed from the glovebox, loaded immediately into the spectrometer and the progress of the reaction monitored by ¹H NMR spectroscopy at the desired temperature (26 °C or 60 °C). The kinetics for rare-earth metal diisopropylamide complexes **1–5** and Ln[N(SiMe₃)₂]₃ (**6**) as catalysts were measured by integrating the intrinsic signals of the educt (H₂C=CH) and product (*H*-2), respectively. The signals of hexamethyldisilazane or diisopropylamine which were formed by protonolysis of the appropriate precatalysts at the beginning of the reactions and stayed unchanged during the catalytic runs were chosen as internal standards. The cyclized amines **P1**, **P2** and **P3** as well as the isomerized aminoalkene **P4** were identified by ¹H NMR spectroscopy (NMR resonances included in the ESI†), the chemical shifts comparable to those described in literature.^{36,57}

Acknowledgements

We thank the German Science Foundation (Grant AN 238/16-1) for funding and D. Schneider for a sample of Ce(NiPr₂)₄.

Notes and references

- 1 T. E. Müller and M. Beller, *Chem. Rev.*, 1998, **98**, 675.
- 2 S. Hong and T. J. Marks, *Acc. Chem. Res.*, 2004, **37**, 673.
- 3 T. E. Müller, K. C. Hultzsch, M. Yus, F. Foubelo and M. Tada, *Chem. Rev.*, 2008, **108**, 3795.
- 4 (a) A. L. Reznichenko and K. C. Hultzsch, *Struct. Bonding*, 2010, **137**, 1; (b) A. L. Reznichenko and K. C. Hultzsch, Hydroamination of Alkenes, in *Organic Reactions*, Wiley, Hoboken, NJ, 2016, pp. 1–554.
- 5 (a) P. W. Roesky and T. E. Müller, *Angew. Chem., Int. Ed.*, 2003, **42**, 2708; (b) J. Hannouche and E. Schulz, *Chem. – Eur. J.*, 2013, **19**, 4972.
- 6 (a) M. R. Gagne and T. J. Marks, *J. Am. Chem. Soc.*, 1989, **111**, 4108; (b) M. R. Gagne, C. L. Stern and T. J. Marks, *J. Am. Chem. Soc.*, 1992, **114**, 275.
- 7 (a) M. R. Bürgstein, H. Berberich and P. W. Roesky, *Organometallics*, 1998, **17**, 1452; (b) M. Rastatter, A. Zulys and P. W. Roesky, *Chem. Commun.*, 2006, 874; (c) M. Rastatter, A. Zulys and P. W. Roesky, *Chem. – Eur. J.*, 2007, **13**, 3606; (d) H. F. Yuen and T. J. Marks, *Organometallics*, 2008, **27**, 155; (e) L. J. E. Stanlake and L. L. Schafer, *Organometallics*, 2009, **28**, 3990; (f) A. Otero, A.- Lara-Sánchez, J. A. Castro-Osma, I. Márquez-Segovia, C. Alonso-Moreno, J. Fernández-Baeza, L. F. Sánchez-Barba and A. M. Rodriguez, *New J. Chem.*, 2015, **39**, 7672.
- 8 (a) Y. K. Kim and T. Livinghouse, *Angew. Chem., Int. Ed.*, 2002, **41**, 3645; (b) Y. K. Kim, T. Livinghouse and Y. Horino, *J. Am. Chem. Soc.*, 2003, **125**, 9560; (c) Y. K. Kim, T. Livinghouse and J. E. Bercaw, *Tetrahedron Lett.*, 2001, **42**, 2933; (d) J. Y. Kim and T. Livinghouse, *Org. Lett.*, 2005, **7**, 4391; (e) C. Quinet, A. Ates and I. E. Markó, *Tetrahedron Lett.*, 2008, **49**, 5032; (f) J. Y. Kim and T. Livinghouse, *Org. Lett.*, 2005, **7**, 1737; (g) X. Yu and T. J. Marks, *Organometallics*, 2007, **26**, 365; (h) T. Jiang and T. Livinghouse, *Org. Lett.*, 2010, **12**, 4271.
- 9 S. Hong, S. Tian, M. V. Metz and T. J. Marks, *J. Am. Chem. Soc.*, 2003, **125**, 14768.
- 10 P. N. O'Shaughnessy, K. M. Gillespie, P. D. Knight, I. J. Munslow and P. Scott, *Dalton Trans.*, 2004, 2251.
- 11 D. V. Gribkov, K. C. Hultzsch and F. Hampel, *J. Am. Chem. Soc.*, 2006, **128**, 3748.
- 12 (a) Y. Zhang, W. Yao, H. Li and Y. Mu, *Organometallics*, 2012, **31**, 4670; (b) Z. Chai, D. Hua, K. Li, J. Chu and G. Yang, *Chem. Commun.*, 2014, **50**, 177 and references therein.
- 13 A. L. Reznichenko, A. J. Nawara-Hultzsch and K. C. Hultzsch, *Top. Curr. Chem.*, 2014, **343**, 191–260.
- 14 (a) A. L. Reznichenko, H. N. Nguyen and K. C. Hultzsch, *Angew. Chem., Int. Ed.*, 2010, **49**, 8984; (b) A. L. Reznichenko and K. C. Hultzsch, *Organometallics*, 2013, **32**, 1394.
- 15 M. R. Bürgstein, H. Berberich and P. W. Roesky, *Chem. – Eur. J.*, 2001, **7**, 3078.
- 16 E. L. Roux, Y. Liang, M. P. Storz and R. Anwander, *J. Am. Chem. Soc.*, 2010, **132**, 16368.

17 K. C. Hultzsch, F. Hampel and T. Wagner, *Organometallics*, 2004, **23**, 2601.

18 (a) M. A. Giardello, V. P. Conticello, L. Brard, M. Sabat, A. L. Rheingold, C. L. Stern and T. J. Marks, *J. Am. Chem. Soc.*, 1994, **116**, 10212; (b) M. A. Giardello, V. P. Conticello, L. Brard, M. R. Gagne and T. J. Marks, *J. Am. Chem. Soc.*, 1994, **116**, 10241.

19 J. Eppinger, M. Spiegler, W. Hieringer, W. A. Herrmann and R. Anwander, *J. Am. Chem. Soc.*, 2000, **122**, 3080.

20 R. R. Fraser, M. Bresse and T. S. Mansour, *J. Chem. Soc., Chem. Commun.*, 1983, 620.

21 T. Spallek, O. Hefß, M. Meermann-Zimmermann, C. Meermann, M. G. Klimpel, F. Estler, D. Schneider, W. Scherer, M. Tafipolsky, K. W. Törnroos, C. Maichle-Mössmer, P. Sirsch and R. Anwander, *Dalton Trans.*, 2016, **45**, 13750.

22 L. Ackermann, L. T. Kaspar and A. Althammer, *Org. Biomol. Chem.*, 2007, **5**, 1975.

23 A. Ates and C. Quinet, *Eur. J. Org. Chem.*, 2003, 1623.

24 C. Quinet, P. Jourdain, C. Hermans, A. Ates, I. Lucas and I. E. Markó, *Tetrahedron*, 2008, **64**, 1077.

25 P. N. O'Shaughnessy and P. Scott, *Tetrahedron: Asymmetry*, 2003, **14**, 1979.

26 D. Riegert, J. Collin, J.-C. Daran, T. Fillebeen, E. Schulz, D. Lyubov, G. Fukin and A. Trifonov, *Eur. J. Inorg. Chem.*, 2007, **2007**, 1159.

27 (a) J. Collin, J. C. Daran, E. Schulz and A. Trifonov, *Chem. Commun.*, 2003, 3048; (b) J. Collin, J. C. Daran, O. Jacquet, E. Schulz and A. Trifonov, *Chem. – Eur. J.*, 2005, **11**, 3455; (c) D. Riegert, J. Collin, A. Meddour, E. Schulz and A. Trifonov, *J. Org. Chem.*, 2006, **71**, 2514; (d) I. Aillaud, K. Wright, J. Collin, E. Schulz and J.-P. Mazaleyrat, *Tetrahedron: Asymmetry*, 2008, **19**, 82.

28 I. Aillaud, J. Collin, C. Duhayon, R. Guillot, D. Lyubov, E. Schulz and A. Trifonov, *Chem. – Eur. J.*, 2008, **14**, 2189.

29 Y. Chapurina, R. Guillot, D. Lyubov, A. Trifonov, J. Hannedouche and E. Schulz, *Dalton Trans.*, 2013, **42**, 507.

30 K₂Ca anilide ate complexes catalyze the intermolecular hydroamination of butadiynes: (a) C. Glock, H. Görls and M. Westerhausen, *Chem. Commun.*, 2012, **48**, 7094; (b) F. M. Younis, S. Krieck, H. Görls and M. Westerhausen, *Organometallics*, 2015, **34**, 3577 and references therein.

31 G. R. Giesbrecht, G. E. Collis, J. C. Gordon, D. L. Clark, B. L. Scott and N. J. Hardman, *J. Organomet. Chem.*, 2004, **689**, 2177.

32 M. Arrowsmith, M. S. Hill and G. Kociok-Köhn, *Organometallics*, 2014, **33**, 206.

33 R. M. Beesley, C. K. Ingold and J. F. Thorpe, *J. Chem. Soc., Dalton Trans.*, 1915, **107**, 1080.

34 M. E. Jung and G. Piizi, *Chem. Rev.*, 2005, **105**, 1735.

35 J. E. Baldwin, *J. Chem. Soc., Chem. Commun.*, 1976, 734.

36 (a) M. R. Crimmin, M. Arrowsmith, A. G. M. Barrett, I. J. Casely, M. S. Hill and P. A. Procopiou, *J. Am. Chem. Soc.*, 2009, **131**, 9670; (b) J. Jenter, R. Köppe and P. W. Roesky, *Organometallics*, 2011, **30**, 1404.

37 For representative examples of α -olefin isomerization at Ln(III) centres, see: (a) E. Bubel, B. J. Burger and J. E. Bercaw, *J. Am. Chem. Soc.*, 1988, **110**, 976; (b) C. Qian, Y. Ge, D. Deng, Y. Gu and C. Zhang, *J. Organomet. Chem.*, 1988, **344**, 175.

38 S. Harder, *Chem. Rev.*, 2010, **110**, 3852.

39 R. Shannon, *Acta Crystallogr., Sect. A: Fundam. Crystallogr.*, 1976, **32**, 751.

40 R. D. Closson, J. P. Napolitano, G. G. Ecke and A. J. Kolka, *J. Org. Chem.*, 1957, **22**, 646.

41 G. P. Pez and J. E. Galle, *Pure Appl. Chem.*, 1985, **57**, 1917.

42 (a) B. M. Trost and W. Tang, *J. Am. Chem. Soc.*, 2002, **124**, 14542; (b) B. M. Trost and W. Tang, *J. Am. Chem. Soc.*, 2003, **125**, 8744.

43 (a) T. Ogata, A. Ujihara, S. Tsuchida, T. Shimizu, A. Kaneshige and K. Tomioka, *Tetrahedron Lett.*, 2007, **48**, 6648; (b) S. Tsuchida, A. Kaneshige, T. Ogata, H. Baba, Y. Yamamoto and K. Tomioka, *Org. Lett.*, 2008, **10**, 3635.

44 P. Horrillo-Martínez, K. C. Hultzsch, A. Gil and V. Branchadell, *Eur. J. Org. Chem.*, 2007, 3311.

45 P. H. Martinez, K. C. Hultzsch and F. Hampel, *Chem. Commun.*, 2006, 2221.

46 I. Aillaud, D. Lyubov, J. Collin, R. Guillot, J. Hannedouche, E. Schulz and A. Trifonov, *Organometallics*, 2008, **27**, 5929.

47 Y. Chapurina, J. Hannedouche, J. Collin, R. Guillot, E. Schulz and A. Trifonov, *Chem. Commun.*, 2010, **46**, 6918.

48 Y. Chapurina, H. Ibrahim, R. Guillot, E. Kolodziej, J. Collin, A. Trifonov, E. Schulz and J. Hannedouche, *J. Org. Chem.*, 2011, **76**, 10163.

49 C. Meermann, G. Gerstberger, M. Spiegler, K. W. Törnroos and R. Anwander, *Eur. J. Inorg. Chem.*, 2008, 2014.

50 F. Estler, G. Eickerling, E. Herdtweck and R. Anwander, *Organometallics*, 2003, **22**, 1212.

51 D. Schneider, T. Spallek, C. Maichle-Mössmer, K. W. Törnroos and R. Anwander, *Chem. Commun.*, 2014, **50**, 14763.

52 For examples of Ce(IV)-promoted homogeneous catalysis, see: (a) I. E. Markó, A. Ates, A. Gautier, B. Leroy, J.-M. Plancher, Y. Quesnel and J.-C. Vanherck, *Angew. Chem., Int. Ed.*, 1999, **38**, 3207; (b) K. K. Laali, M. Herbert, B. Cushnyr, A. Bhatt and D. Terrano, *J. Chem. Soc., Perkin Trans. 1*, 2001, 578; (c) N. Nomura, A. Tiara, A. Nakase, T. Tomioka and M. Okada, *Tetrahedron*, 2007, **63**, 8478; (d) E. M. Broderick and P. L. Diaconescu, *Inorg. Chem.*, 2009, **48**, 4701; (e) A. Sauer, J.-C. Buffet, T. P. Spaniol, H. Nagae, K. Maschima and J. Okuda, *ChemCatChem*, 2013, **5**, 1088; (f) H. Yin, P. J. Carroll, B. C. Manor, J. M. Anna and E. J. Schelter, *J. Am. Chem. Soc.*, 2016, **138**, 5984.

53 H. K. Hall, *J. Am. Chem. Soc.*, 1957, **79**, 5441.

54 F. Lauterwasser, P. G. Hayes, S. Bräse, W. E. Piers and L. L. Schafer, *Organometallics*, 2004, **23**, 2234.



55 (a) E. C. Alyea, D. C. Bradley and R. G. Copperthwaite, *J. Chem. Soc., Dalton Trans.*, 1972, 1580; (b) D. C. Bradley, J. S. Ghotra and F. A. Hart, *J. Chem. Soc., Chem. Commun.*, 1972, 349; (c) D. C. Bradley, J. S. Ghotra and F. A. Hart, *J. Chem. Soc., Dalton Trans.*, 1973, 1021.

56 W. Bauer and D. Seebach, *Helv. Chim. Acta*, 1984, **67**, 1972.

57 M. Arrowsmith, M. R. Crimmin, A. G. M. Barrett, M. S. Hill, G. Kociok-Köhn and P. A. Procopiou, *Organometallics*, 2011, **30**, 1493.

